A conservative model for unsteady flows in deformable closed pipes and its implicit second order finite volume discretisation.

C. Bourdarias, S. Gerbi

Université de Savoie, LAMA, GM^3*, 73376 Le Bourget-du-Lac Cedex, France.*

Abstract

We present a one dimensional model for compressible flows in a deformable pipe which is an alternative to the Allievi equations and is intended to be coupled in a "natural way" with the shallow water equations to simulate mixed flows. The numerical simulation is performed using a second order linearly implicit scheme adapted from the Roe scheme. The validation is performed in the case of water hammer in a rigid pipe: we compare the numerical results provided by an industrial code with those of our spatial second order implicit scheme. It appears that the maximum value of the pressure within the pipe for large CFL numbers and a coarse discretisation is accurately computed.

Key words: pressurised flows, water hammer, implicit schemes, Roe scheme, boundary conditions,

1 Introduction

The work presented in this article is the first step in a more general project: the modelisation of unsteady mixed flows in open channels and in pipes and its finite volume discretisation. Since we are interested in flows occuring in closed pipes it may happen that some parts of the flow are free-surface (this means that only a part of the cross-section of the pipe is filled) and other parts are pressurised (this means that all the cross-section of the pipe is filled). The Saint Venant equations, which are written in a conservative form, are usually used to describe free surface flows of water in open channels. They are also

Email address: christian.bourdarias@univ-savoie.fr, stephane.gerbi@univ-savoie.fr (C. Bourdarias, S. Gerbi).

used in the context of mixed flows using the artifice of the Preissman slot [19],[5] : Cunge and Wegner [6] studied the pressurised flow in the pipe as if it were a free-surface flow by assuming a narrow slot to exist in the upper part of the pipe, the width of the slot being calculated to provide the correct sonic speed. This approach has been credited to Preissmann. Implementing the Preissmann slot technique has the advantage of using only one flow type (free-surface flow) throughout the whole pipe and of being able to easily quantify the pressure head when the pipe pressurises. Nevertheless, as pointed out by several authors (see [18] for instance) the pressurising phenomenon is a dynamic shock requiring a full dynamic treatment even if inflows and other boundary conditions change very slowly. In addition, the Preissmann slot technique is unable to take into account the depressurisation phenomenon which occurs during a waterhammer.

The commonly used model to describe pressurised flows in pipe-lines is the system of Allievi equations. These equations are usually solved with the characteristics method (see [20] for instance). The resulting system of first order partial differential equations is not written under a conservative form since this model is derived by neglecting some acceleration terms. This non conservative formulation is not appropriate for a finite volume discretization. Above all, it appears that a "unified" modelisation with a common set of conservative variables (see below) could be of a great interest for the coupling between free-surface and pressurised flows and its numerical simulation could be more effective.

In this paper, we derive a 1D model from 3D compressible Euler equations by integration over sections orthogonal to the flow direction and by using a linearized pressure law. We will consider entirely rigid as well as deformable pipes (through the use of a Hooke's law for the deformation of the pipe due to the change of pressure). This model is a 1D first order hyperbolic system of partial differential equations written in conservative form which is formally very close to the Saint-Venant equations for shallow water. This particular fact is used to derive a model and a numerical scheme for mixed flows in an article (in press at the present time) [2]. The goal of the present paper is essentially to build the new model for pressurised flows, to describe a finite volume discretisation and to carry out a code to code validation by the resolution of standard critical tests of waterhammer.

The paper is organised as follows. In section 2, we present a formal derivation of the model from 3D compressible Euler equations. Section 3 is devoted to the finite volume discretisation of the proposed model. Since the CFL condition for explicit scheme is very restrictive, we choose, following [11,8], to discretise the system of first order conservative partial differential equations by a linear implicit finite volume scheme to avoid the usual CFL condition for an explicit spatial discretization. For the boundary condition treatment, we propose an

adaptation of a classical method ([7,14] for instance) to the implicit case. We recall the principle of the first order explicit Roe scheme and then we adapt it to build a linearly implicit method. Then the method to build the "missing" boundary conditions is described, and the second order MUSCL scheme is formulated. Finally in section 4, we present the numerical validation of this study by the comparison between the resolution of this model and the resolution of the Allievi equation solved by the research code `belier` used at Center in Hydraulics Engineering of Electricité De France (EDF) [21] for the case of critical waterhammer tests.

2 Formal derivation of the model

This model is derived from 3D system of compressible Euler equations by integrating over sections orthogonal to the flow axis. Hence, we neglect the second and third equation for the conservation of the momentum. In the cartesian coordinate system (shown in the figure 1), where the vector $\vec{i}$ is along the pipe axis, the equation for conservation of mass and the first equation for the conservation of momentum are:

$$\partial_t \rho + \mathrm{div}(\rho \vec{U}) = 0 \tag{1}$$

$$\partial_t(\rho u) + \mathrm{div}(\rho u \vec{U}) = F_x - \partial_x P \tag{2}$$

with the speed vector $\vec{U} = u\vec{i} + v\vec{j} + w\vec{k} = u\vec{i} + \vec{V}$. We use the linearized pressure law:

$$P = P_a + \frac{\rho - \rho_0}{\beta \rho_0} \tag{3}$$

in which ρ represents the density of the liquid, ρ_0, the density at atmospheric pressure P_a and β the water compressibility coefficient (which is the inverse of the bulk modulus of elasticity). The sound speed is then given by:

$$c = \frac{1}{\beta \rho_0} \quad . \tag{4}$$

Practically, $\beta = 5.0\ 10^{-10}$ m^2/N and thus $c \simeq 1400$ m/s.

Exterior strengths, with x-component F_x, are the gravity $\vec{g}$ and the friction $-\rho g S_f \vec{i}$ given by the Manning-Strickler law (see [19]),

$$S_f = K(A)\, u\, |\, u\, | \text{ with } K(A) = \frac{1}{K_s^2\, R_h(A)^{4/3}}$$

where $A = A(x,t)$ is the given surface area of a section $\Omega(x,t)$ normal to the pipe axis at position x and at time t, (see Fig. 1), $K_s > 0$ is the Strickler

coefficient of roughness and $R_h(A)$ is the so called hydraulic radius given by $R_h(A) = \dfrac{A}{P_m}$, P_m being the perimeter of Ω. For instance, in the case of a fully-filled circular pipe with diameter δ we get $R_h = \delta/4$.

Then equations (1)-(2) become

$$\partial_t \rho + \partial_x(\rho\, u) + \mathrm{div}_{(y,z)}(\rho\, \vec{V}) = 0 \tag{5}$$

$$\partial_t(\rho\, u) + \partial_x(\rho\, u^2) + \mathrm{div}_{(y,z)}(\rho\, u\, \vec{V}) = \rho g(\sin\theta - S_f) - c^2\, \partial_x \rho \tag{6}$$

Equations (5)-(6) are integrated over a cross-section $\Omega(x,t)$ (Fig.1, left).

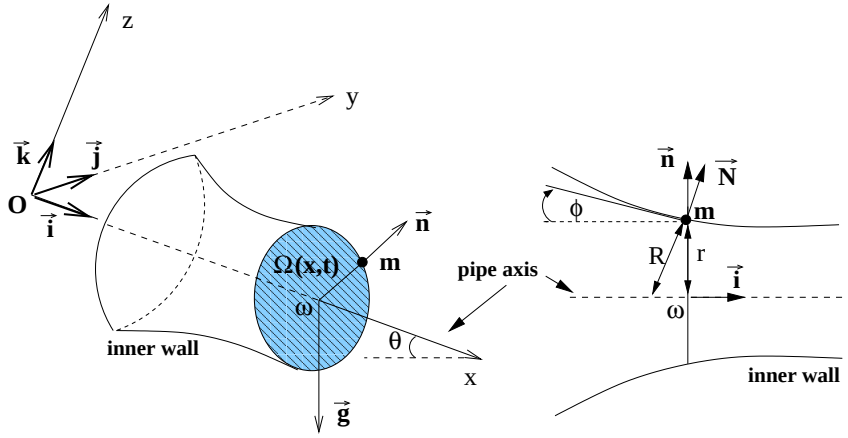

Fig. 1. *Geometric characteristics of the pipe.*

In the following, overlined letters represent averaged quantities over $\Omega(x,t)$. For equation (5) we have successively, with the approximation $\overline{\rho u} \simeq \overline{\rho}\,\overline{u}$:

$$\int\limits_{\Omega(x,t)} \partial_t \rho = \partial_t \int\limits_{\Omega(x,t)} \rho - \int\limits_{\partial\Omega(x,t)} \rho\ \partial_t \vec{m} \cdot \vec{n},$$

where $m \in \partial\Omega$, $\vec{m}$ stands for $\overrightarrow{Om}$ and $\vec{n} = \dfrac{\vec{m}}{|\vec{m}|}$ is the outward unit vector at the point m in the Ω-plane (see Fig. 1),

$$\int\limits_{\Omega(x,t)} \partial_x(\rho\, u) = \partial_x(\overline{\rho}\,\overline{u}\, A) - \int\limits_{\partial\Omega(x,t)} \rho\, u\ \partial_x \vec{m} \cdot \vec{n},$$

$$\int\limits_{\Omega(x,t)} \mathrm{div}_{(y,z)}(\rho\, \vec{V}) = \int\limits_{\partial\Omega(x,t)} \rho\, \vec{V} \cdot \vec{n}.$$

Therefore we get the following equation for the conservation of the mass:

$$\partial_t(\overline{\rho}A) + \partial_x(\overline{\rho}\,\overline{Q}) = \int\limits_{\partial\Omega(x,t)} \rho\,\left(\partial_t\vec{m} + u\,\partial_x\vec{m} - \vec{V}\right)\cdot\vec{n}\;, \tag{7}$$

where we have set $\overline{Q} = A\,\overline{u}$ the discharge of the flow.

Next, with the approximations $\overline{\rho u} \simeq \overline{\rho}\,\overline{u}$ and $\overline{\rho u^2} \simeq \overline{\rho}\,\overline{u}^2$, we get for the equation (6):

$$\int\limits_{\Omega(x,t)} \partial_t(\rho\,u) = \partial_t \int\limits_{\Omega(x,t)} \rho\,u - \int\limits_{\partial\Omega(x,t)} \rho\,u\,\partial_t\vec{m}\cdot\vec{n} = \partial_t(\overline{\rho}\,\overline{Q}) - \int\limits_{\partial\Omega(x,t)} \rho\,u\,\partial_t\vec{m}\cdot\vec{n},$$

$$\int\limits_{\Omega(x,t)} \partial_x(\rho\,u^2) = \partial_x \int\limits_{\Omega(x,t)} \rho\,u^2 - \int\limits_{\partial\Omega(x,t)} \rho\,u^2\,\partial_x\vec{m}\cdot\vec{n} = \partial_x(\overline{\rho}\,\overline{u}^2\,A) - \int\limits_{\partial\Omega(x,t)} \rho\,u^2\,\partial_x\vec{m}\cdot\vec{n},$$

$$\int\limits_{\Omega(x,t)} \mathrm{div}_{(y,z)}(\rho\,u\,\vec{V}) = \int\limits_{\partial\Omega(x,t)} \rho\,u\,\vec{V}\cdot\vec{n},$$

$$c^2 \int\limits_{\Omega(x,t)} \partial_x\rho = c^2\,\partial_x \int\limits_{\Omega(x,t)} \rho - c^2 \int\limits_{\partial\Omega(x,t)} \rho\,\partial_x\vec{m}\cdot\vec{n} = c^2\,\partial_x(\overline{\rho}\,A) - c^2\,\overline{\rho}\,\partial_x A$$

Thus the equation (6) becomes the equation for the conservation of momentum:

$$\begin{aligned}\partial_t(\overline{\rho}\,\overline{Q}) + \partial_x\left(\overline{\rho}\,\frac{\overline{Q}^2}{A} + c^2\,\overline{\rho}\,A\right) &= g\,\overline{\rho}\,A(\sin\theta - S_f) + c^2\,\overline{\rho}\,\partial_x A + \\ &+ \int\limits_{\partial\Omega(x,t)} \rho\,u\,\left(\partial_t\vec{m} + u\,\partial_x\vec{m} - \vec{V}\right)\cdot\vec{n}\end{aligned} \tag{8}$$

To treat the integral terms appearing in equations (7) and(8), we use the no-leak condition at the tube wall $\partial\Omega$ which writes:

$$\vec{U}\cdot\vec{N} = \partial_t\vec{m}\cdot\vec{N},$$

where $\vec{N}$ is the outward unit vector at the point m. It means that the normal velocity of the water at the point $m \in \partial\Omega$ and the normal velocity of m (due to the deformation of the pipe under pressure rise or decrease) are the same. Thus, in the present case of axial symmetry, an easy computation gives:

$$\left(\partial_t\vec{m} + u\,\partial_x\vec{m} - \vec{V}\right)\cdot\vec{n} = (\partial_x r)\,(\partial_t\vec{m}\cdot\vec{i}) \simeq \tan\phi\;(\partial_t\vec{m}\cdot\vec{i})$$

where $r = \omega m = r(x,t)$ is the radius of Ω and $\phi = (\vec{n},\vec{N}) \in]-\pi/2,\,\pi/2[$, with the orientation given by $(\vec{i},\vec{n})$ (see Fig 1, right). For instance we have $\tan\phi < 0$ in contracting sections. On the other hand, neglecting the tangential deformations in the longitudinal sections of the pipe, we set $\partial_t\vec{m} = (\partial_t R)\,\vec{N}$ where $R = R(x,t)$ is the radius of normal curvature at the point m along $\partial\Omega$

(see Fig. 1, right) satisfying $R = r/\cos\phi$. Neglecting the time variations of ϕ, this leads to $\partial_t \vec{m} \cdot \vec{i} = -\dfrac{\tan\phi}{\pi\,\delta}\,\partial_t A$ and we get :

$$\int\limits_{\partial\Omega(x,t)} \begin{pmatrix} \rho \\ \rho\,u \end{pmatrix} \left(\partial_t \vec{m} + u\,\partial_x \vec{m} - \vec{V}\right) \cdot \vec{n} \simeq \frac{1}{A} \begin{pmatrix} \overline{\rho}\,A \\ \overline{\rho}\,\overline{Q} \end{pmatrix} (-\tan^2\phi)\,\partial_t A.$$

Using $\tan\phi = \dfrac{1}{2}\,\partial_x \delta_0$, where δ_0 is the diameter at rest, omitting the overlined notations and setting the conservative variables: $M = \rho\,A$ and $D = \rho\,Q$, the equation (7) for the conservation of the mass becomes:

$$\partial_t(M) + \partial_x(D) = -\frac{1}{4}\frac{\partial_t A}{A}\,(\partial_x \delta_0)^2\,M. \tag{9}$$

To treat the term $\partial_t A$, we use a linear elastic law for the deformation of the section due to the change of pressure, derived from the Hooke's law for an elastic material: $dR = \dfrac{R^2}{e\,E}\,dP$. Setting

$$A = A(x,t) = S(x, P(x,t)), \tag{10}$$

for a pipe with a circular cross-section, this law writes (see [19] for instance, in the case of a constant radius):

$$\frac{\partial S}{\partial P} = \frac{S\delta}{e\,E\,\cos\phi} \tag{11}$$

where $\delta = \delta(x,t)$ is the diameter of the pipe, e is the wall thickness (assumed to be a constant for the sake of simplicity), E is the Young's modulus of elasticity for the wall material. $\phi = \phi(x)$ is the angle $(\vec{n}, \vec{N})$ between the outward unit vector of the cross-section Ω at a point m of the inner wall of the pipe and the outward unit vector $\vec{N}$ at the same point (see Fig. 1, right side). It is assumed to be constant in time for the sake of simplicity.

From (10) and (11) we get

$$\partial_x A = \partial_x S + \frac{A\,\delta}{e\,E\,\cos\phi}\,\partial_x P$$

and then, using (3), the term $c^2\,\rho\,\partial_x A$ in (8) writes:

$$\begin{aligned} c^2\,\rho\,\partial_x A &= c^2\,\rho\,\frac{\delta}{e\,E\,\cos\phi}\,A\,\partial_x \rho + c^2\,\rho\,\partial_x S \\ &= c^4\,\rho\,\frac{\delta}{e\,E\,\cos\phi}\,\partial_x(\rho\,A) - c^4\,\rho^2\,\frac{\delta}{e\,E\,\cos\phi}\,\partial_x A + c^2\,\rho\,\partial_x S \end{aligned}$$

This leads easily to

$$c^2\,\rho\,\partial_x A = \partial_x((c^2 - a^2)\,\rho\,A) + a^2\,\rho\,\partial_x S + \rho\,A\,\partial_x a^2$$

with a given by $\dfrac{c}{\sqrt{1 + \dfrac{\rho}{\rho_0}\dfrac{\delta}{\beta\,e\,E\,\cos\phi}}}$ (for a circular pipe) and approximated by:

$$a = a(x,t) = \frac{c}{\sqrt{1 + \dfrac{\delta(x,t)}{\beta\,e\,E\,\cos\phi(x)}}} \quad . \tag{12}$$

a represents the speed of sound for the considered pipe and takes into account the deformation of the pipe (by the dependancy in time) and also the non-uniformness of the pipe by the dependancy in the diameter at the position x. In the infinitely rigid case ($E = +\infty$), we recover the speed of sound c given by the equation (4) whereas in the rigid case for a non-uniform pipe, we must take into account the variation of the section with respect to the position x and thus the variation of the speed of the sound $\partial_x a$.

The term $\partial_x S$ is approximated by $\partial_x S_0$ where S_0 is the area of the cross-section at rest ($S_0(x) = S(x, P_a)$). Thus the equation (8) for the conservation of the momentum becomes:

$$\begin{aligned}\partial_t(D) + \partial_x\left(\frac{D^2}{M} + a^2\,M\right) = g\,M\,\sin\theta(x) - g\,K(A)\,\frac{D|D|}{M} + M\,\partial_x a^2 + \\ + a^2\,\frac{M}{A}\,\partial_x S_0 - \frac{1}{4}\frac{\partial_t A}{A}\,(\partial_x \delta_0)^2\,D\end{aligned} \tag{13}$$

Lastly, proceeding for $\partial_t A$ in the same way as for $\partial_x A$, we get:

$$\partial_t A = k\,\partial_t M \tag{14}$$

with $k = k(x,t) = \dfrac{\delta(x,t)}{e\,E\,\cos\phi(x)}\,a(x,t)^2$.

We can now formulate the system of coupled first order hyperbolic partial differential equation obtained for the two following cases :

For a rigid pipe

$$\partial_t U + \partial_x F(U) = G_r(x,U) \tag{15}$$

where

$$U = (\rho\,A\ ,\ \rho\,Q)^t = (M\ ,\ D)^t \quad , \quad F(U) = \left(D\ ,\ \frac{D^2}{M} + a(x)^2\,M\right)^t$$

and the source term G_r writes:

$$G_r(x,U) = \left(0\ ,\ g\,M\,\sin\theta(x) - g\,K(A)\,\frac{D|D|}{M} + M\,\partial_x a^2 + a(x)^2\,\frac{M}{A}\,\partial_x S_0\right)^t \tag{16}$$

For a deformable pipe

$$\partial_t U + \partial_x F(U) = G_d(x,U) \tag{17}$$
$$\partial_t A = k\,\partial_t M \tag{18}$$

where

$$U = (\rho A\ ,\ \rho Q)^t = (M\ ,\ D)^t \quad , \quad F(U) = \left(D\ ,\ \frac{D^2}{M} + a(x)^2\,M\right)^t$$

and the source term G_d writes :

$$G_d(x,U) = G_r - \frac{1}{4}\frac{\partial_t A}{A}\ (\partial_x \delta_0)^2\ U \tag{19}$$

Let us mention that the above model is formally close to the system of Saint-Venant for shallow water, where the unknown state vector U and the flux $F(U)$ are given by:

$$U = (A\ ,\ Q)^t \quad \text{and} \quad F(U) = \left(Q\ ,\ \frac{Q^2}{A} + g\,I_1(A)\right)^t,$$

$A = A(x,t)$ being the so-called wetted area and $g\,I_1(A)$ arising from the hydrostatic pressure law. Then a common set of conservative variables is for instance $U = \left(A_{eq} = \frac{\rho A}{\rho_0}\ , Q_{eq} = \frac{\rho Q}{\rho_0}\right)^t$ ("free surface -equivalent area" and "free surface -equivalent discharge"). The two models mainly differ by the pressure law. It is the reason why it seems natural to formulate the mixed flow problems as a first order hyperbolic system of partial differential equations with discontinuities (in the gradient of the pressure) located at the interface between the two types of flows (free surface/pressurised). The modelisation, the treatment of this type of discontinuity, the numerical results and the experimental validation will be presented in a forthcoming paper [4,2].

3 The finite volume discretisation and its implicit formulation

For the numerical approximation of (9), (13), (14) with suitable initial and boundary conditions, we use a finite volume method with a Roe-like numerical flux in a partial linear implicit version. We present here a second order extension of the implicit first order scheme described in [3] and adapted to a pipe with contracting or expanding sections.

The main axis of the pipe, with length L, is divided in N meshes $m_i = [x_{i-1/2}, x_{i+1/2}]$, $1 \leq i \leq N$ such that $x_{\frac{1}{2}} = 0$ and $x_{N+\frac{1}{2}} = L$. We denote by x_i the center of m_i and by h_i its length. Δt denotes the timestep. We set $t_0 = 0$ and for $n \geq 0$, $t_{n+1} = t_n + \Delta t$. The discrete unknowns are $U_i^n = \begin{pmatrix} M_i^n \\ D_i^n \end{pmatrix}$, $1 \leq i \leq N$, $0 \leq n \leq n_{max}$ that approximate the mean value of $U(x,t)$ on $m_i \times [t_n, t_{n+1}]$, and A_i^n that approximates $A(x_i, t_n)$. The upstream and downstream boundary states U_0^n, U_{N+1}^n are associated to fictive meshes denoted 0 and $N+1$.
Let R be a diagonalizable $d \times d$ real matrix with real eigenvalues $\lambda_1, \cdots \lambda_d$ associated to eigenvectors $r_1, \cdots, r_d$: $\mathrm{diag}(\lambda_i) = P^{-1} M P$. We set $|R| = P\,\mathrm{diag}(|\lambda_i|)\,P^{-1}$ ("absolute value" of the matrix R).

3.1 Principle of explicit 1st order Roe scheme. Well balanced VF-Roe scheme

In this section we recall the principle of the explicit first order Roe scheme and explain how to bypass the difficulties which arise in the case of a deformable pipe and/or a non uniform geometry.

Roe's scheme, derived from Godunov's method, is based on the use of an approximate Riemann solver (see [8] for instance). It takes the conservative form:

$$\frac{U_i^{n+1} - U_i^n}{\Delta t} + \frac{F_{i+1/2}^n - F_{i-1/2}^n}{h_i} = G_i^n \quad 1 \leq i \leq N, \quad n \geq 0. \tag{20}$$

For all $1 \leq i \leq N$, U_i^0 is computed as the averaged value of the initial data U_0 on the mesh m_i. The right hand side G_i^n is a centered approximation of the contribution of the source terms in the mesh m_i, the numerical flux $F_{i+1/2}^n$ is given by $F_{i+1/2}^n = F(U_{i+1/2}^*(0, U_i^n, U_{i+1}^n))$ where $U_{i+1/2}^*(\xi, U_l, U_r)$ is the exact solution, along the line $\xi = x/t$, of the linearized Riemann problem:

$$(PRL) \qquad \begin{cases} \dfrac{\partial U}{\partial t} + R(U_l, U_r)\dfrac{\partial U}{\partial x} = 0 \\ U(x,0) = \begin{cases} U_l & \text{if } x < 0, \\ U_r & \text{if } x > 0, \end{cases} \end{cases}$$

the function R with values in the set of 2×2 real matrices being subject to the conditions

(1) R is continuous,
(2) $R(U_l, U_r) \cdot (U_l - U_r) = F(U_l) - F(U_r)$ (Roe's condition, ensuring conservativity)
(3) $R(U_l, U_r)$ is diagonalizable with real eigenvalues.

The two first conditions imply $R(U,U) = JF(U)$, Jacobian matrix of the function F (consistency). In its centered form, the numerical flux takes the form:

$$F^n_{i+1/2} = \frac{F(U^n_i) + F(U^n_{i+1})}{2} + \frac{1}{2}|R(U^n_i, U^n_{i+1})| \cdot (U^n_i - U^n_{i+1})$$

The timestep (at time t_n) in the resulting scheme is classically subject to a "Courant-Friedrich-Lévy type" condition:

$$(CFL) \qquad \Delta t \leq C \frac{\inf\limits_{1\leq i\leq N} h_i}{\max\left\{\left|\tilde{\lambda}^n_{k,i+1/2}\right|;\ 1 \leq k \leq 2,\ 1 \leq i \leq N\right\}} \quad C \in]0,1[$$

where $\tilde{\lambda}^n_{k,i+1/2}$ is the k^{th} eigenvalue of the matrix $R(U^n_i, U^n_{i+1})$. C is called the CFL coefficient.
Following Roe's method ([16] in the case of one-dimensional Euler equations) we get, in the case of an entirely rigid pipe, the following Roe matrix:

$$R(U_l, U_r) = \begin{pmatrix} 0 & 1 \\ c^2 - \tilde{u}^2 & 2\tilde{u} \end{pmatrix}, \quad \text{with } \tilde{u} = \frac{u_l\sqrt{M_l} + u_r\sqrt{M_r}}{\sqrt{M_l} + \sqrt{M_r}}.$$

The eigenvalues of $R(U_l, U_r)$ are $\tilde{\lambda}_1 = \tilde{u} - c \quad < 0 < \quad \tilde{\lambda}_2 = \tilde{u} + c$, associated to the right eigenvectors $\tilde{r}_1 = \begin{pmatrix} 1 \\ \tilde{u} - c \end{pmatrix}$ and $\tilde{r}_2 = \begin{pmatrix} 1 \\ \tilde{u} + c \end{pmatrix}$.

In the case of a deformable pipe, we have no longer such a Roe matrix because of the dependency of the sound speed a upon x (via $\cos\phi$ and the diameter δ). Moreover, in the case of a non constant slope and overall in the case of a contracting or expanding section, the centered treatment of the corresponding source terms gives a scheme which is unable to preserve steady states.

Following Gallout ([9]) we can bypass the non existence of a Roe matrix by writing a priori the scheme under the conservative form (20) with $F^n_{i+1/2}$ computed as above, but using a matrix $R(U^n_i, U^n_{i+1}) = JF(\overline{U})$ where $\overline{U}$ is some intermediate state between U^n_i and U^n_{i+1} (for instance $\overline{U} = \frac{U^n_i + U^n_{i+1}}{2}$). This matrix is subject to the conditions 1 and 3 and to the consistency condition $R(U,U) = F(U)$. The corresponding scheme is called a VF-Roe scheme in [9]. We choose this approach, combined with an upwind treatment of the part of the source terms due to both the slope (term $gM\sin\theta$) and the geometry (terms $a^2\,\frac{M}{A}\,\partial_x S_0$ and $M\,\partial_x a^2$).
For the sake of simplicity, we built our first order explicit scheme without

taking in account the time derivative of A (and thus assuming $A = S_0$). The general case is obtained via a straightforward splitting method that we briefly explain at the end of the next subsection.
Following Leroux *et al.* [13,17] we use a piecewise constant function to approximate the bottom of the pipe as well as the area S_0. Let be z the elevation of the pipe axis at position x. Setting

$$Z = z - \frac{a^2}{g} \ln S_0 \quad \text{and} \quad \Psi(x) = \frac{a^2(x)}{c^2}$$

(for the case of circular pipe $\Psi(x) = \left(1 + \dfrac{\delta(x)}{\beta\, e\, E\, \cos\phi(x)}\right)^{-1}$), we first remark that

$$g\, M\, \sin\theta + a^2\, \frac{M}{S_0}\, \partial_x S_0 = -g\, M\, \partial_x Z - M\, (\ln S_0)\, c^2\, \partial_x \Psi. \tag{21}$$

Next, adding the equations $\partial_t Z = 0$ and $\partial_t \Psi = 0$ to the system (9)-(13) and setting

$$W = (Z, \Psi, M, D)^t,$$

we get the following system:

$$\partial_t W + \partial_x \Phi(x, W) + g\, M\, \partial_x Z + M\, (\ln S_0 - 1)\, c^2\, \partial_x \Psi = TS(W) \tag{22}$$

with

$$\Phi(x, W) = \begin{pmatrix} 0 \\ 0 \\ D \\ \dfrac{D^2}{M} + a^2\, M \end{pmatrix} \quad TS(W) = \begin{pmatrix} 0 \\ 0 \\ 0 \\ -g\, K(A)\, \dfrac{D\,|D|}{M} \end{pmatrix}$$

Such an approximation of the topography and the geometry introduces two stationary waves for each local Riemann problem at the interfaces $x_{i+1/2}$. Let W_i^n be an approximation of the mean value of W on the mesh m_i at time t_n. Integrating the above equation (22) over $]x_{i-1/2}, x_{i+1/2}[\times[t_n, t_{n+1}[$ with piecewise constant data at time t_n, we deduce an explicit Finite Volume scheme written as follows:

$$\begin{aligned} W_i^{n+1} = W_i^n - \frac{\Delta t}{h_i} \Big(& \Phi\Big(W^*_{i+1/2}(0^-, W_i^n, W_{i+1}^n)\Big) - \\ & \Phi\Big(W^*_{i-1/2}(0^+, W_{i-1}^n, W_i^n)\Big)\Big) + \\ & + \Delta t\, TS_i^n \end{aligned} \tag{23}$$

where $TS_i^n = TS(W_i^n)$ and $W^*_{i+1/2}(\xi = x/t, W_i^n, W_{i+1}^n)$ is the exact or approximate solution of the Riemann problem at interface $x_{i+1/2}$ associated to

the left and right states W_i^n and W_{i+1}^n. Notice that neither the topography nor the variation of the section and the sound speed appear explicitly in this formulation ($\partial_x Z = 0$ and $\partial_x \Psi = 0$ on $]x_{i-1/2}, x_{i+1/2}[$) but contributes to the computation of the numerical flux. Following Gallouët *et al.* [10] we compute $W^*_{i+1/2}(0^{\pm}, W_i^n, W_{i+1}^n)$ using an approximate Riemann solver of VF-Roe type: let be

$$B(x,W) = \begin{pmatrix} 0 & 0 & 0 & 0 \\ 0 & 0 & 0 & 0 \\ 0 & 0 & 0 & 1 \\ g\,M & c^2 M \ln S_0(x) & a(x)^2 - u^2 & 2\,u \end{pmatrix}$$

the convection matrix associated to the non-conservative form (22), then $W^*_{i+1/2}(\xi = x/t, W_i^n, W_{i+1}^n)$ is the exact solution, along the line $\xi = x/t$, of the linear Riemann problem

$$\begin{cases} \partial_t W + \tilde{J}\,\partial_x W = 0 \\ W = (Z, \Psi, M, D) = \begin{cases} W_i^n = (Z_i, \Psi_i, M_i^n, D_i^n)^t & \text{if } \ x < 0 \\ W_{i+1}^n = (Z_{i+1}, \Psi_{i+1}, M_{i+1}^n, D_{i+1}^n)^t & \text{if } \ x > 0 \end{cases} \end{cases} \tag{24}$$

with $\tilde{J} = \tilde{J}(W_i^n, W_{i+1}^n) = B\left(x_{i+1/2}, \dfrac{W_i^n + W_{i+1}^n}{2}\right)$.

$\tilde{J}$ has the eigenvalues $\tilde{\lambda}_1 = \tilde{\lambda}_2 = 0$, $\tilde{\lambda}_3 = \tilde{u}^n_{i+1/2} - \tilde{a}_{i+1/2}$ and $\tilde{\lambda}_4 = \tilde{u}^n_{i+1/2} + \tilde{a}_{i+1/2}$, with

$$\tilde{u}^n_{i+1/2} = \frac{D_i + D_{i+1}}{M_i + M_{i+1}} \text{ and } \tilde{a}^2_{i+1/2} = \frac{a_i^2 + a_{i+1}^2}{2},\ a_i^2 = c^2\Psi(x_i).$$

The eigenvectors are:

$$\tilde{r}_1 = \begin{pmatrix} \tilde{a}^2_{i+1/2} - (\tilde{u}^n_{i+1/2})^2 \\ 0 \\ -g\,\tilde{M}^n_{i+1/2} \\ 0 \end{pmatrix} \quad \tilde{r}_2 = \begin{pmatrix} c^2\ \ln(S_0)_{i+1/2} \\ -g \\ 0 \\ 0 \end{pmatrix}$$

$$\tilde{r}_3 = \begin{pmatrix} 0 \\ 0 \\ 1 \\ \tilde{u}^n_{i+1/2} - \tilde{a}_{i+1/2} \end{pmatrix} \quad \text{and} \quad \tilde{r}_4 = \begin{pmatrix} 0 \\ 0 \\ 1 \\ \tilde{u}^n_{i+1/2} + \tilde{a}_{i+1/2} \end{pmatrix}$$

with $\tilde{M}^n_{i+1/2} = \dfrac{M_i^n + M_{i+1}^n}{2}$ and $(S_0)_{i+1/2} = S_0(x_{i+1/2})$. The solution of the Riemann problem (24) consists in four constant states connected by shocks

propagating along the lines $\xi = x/t = \lambda_i$. Since the velocity is practically always less (in magnitude) that the sound velocity, we have $-\tilde{a} < \tilde{u} < \tilde{a}$ and then $\tilde{\lambda}_2 < 0 = \tilde{\lambda}_1 < \tilde{\lambda}_3$. Since the values of the "corrected elevation" Z and of Ψ are known, we are looking for the states on each sides of the line $\xi = 0$ denoted by $(M^{n,-}_{i+1/2}, D^{n,-}_{i+1/2})$ for the left side and $(M^{n,+}_{i+1/2}, D^{n,+}_{i+1/2})$ for the right side (see Figure 2 above).

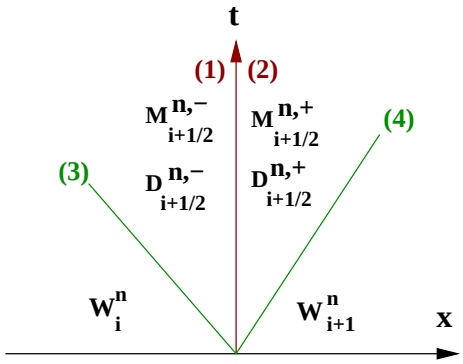

Fig. 2. Solution of the Riemann problem (24). The number of the lines corresponds to those of the eigenvalues.

Moreover, as the third component of $\tilde{r}_1$ is null, the discharge D is continuous through the line $\xi = 0$. Thus $D^{n,-}_{i+1/2} = D^{n,+}_{i+1/2}$. In the sequel, we denote $D^n_{i+1/2}$ this value. A classical computation gives:

$$M^{n,-}_{i+1/2} = M^n_i + \frac{g\,\tilde{M}^n_{i+1/2}}{2\,\tilde{a}_{i+1/2}\,(\tilde{a}_{i+1/2} - \tilde{u}^n_{i+1/2})}\,(Z_{i+1} - Z_i) +$$

$$+ \frac{\tilde{M}^n_{i+1/2}\,\ln(S_0)_{i+1/2}}{2\,\tilde{a}_{i+1/2}\,(\tilde{a}_{i+1/2} - \tilde{u}^n_{i+1/2})}\,(a^2_{i+1} - a^2_i) +$$

$$+ \frac{\tilde{u}^n_{i+1/2} + \tilde{a}_{i+1/2}}{2\,\tilde{a}_{i+1/2}}\,(M^n_{i+1} - M^n_i) -$$

$$- \frac{1}{2\,\tilde{a}_{i+1/2}}\,(D^n_{i+1} - D^n_i)$$

$$D^n_{i+1/2} = D^n_i - \frac{g\,\tilde{M}^n_{i+1/2}}{2\,\tilde{a}_{i+1/2}}\,(Z_{i+1}-Z_i) -$$

$$-\frac{\tilde{M}^n_{i+1/2}\ln(S_0)_{i+1/2}}{2\,\tilde{a}_{i+1/2}}\,(a^2_{i+1}-a^2_i) +$$

$$+\frac{(\tilde{u}^n_{i+1/2})^2-\tilde{a}^2_{i+1/2}}{2\,\tilde{a}_{i+1/2}}\,(M^n_{i+1}-M^n_i) -$$

$$-\frac{\tilde{u}^n_{i+1/2}-\tilde{a}_{i+1/2}}{2\,\tilde{a}_{i+1/2}}\,(D^n_{i+1}-D^n_i)$$

$$M^{n,+}_{i+1/2} = M^{n,-}_{i+1/2} + \frac{g\,\tilde{M}^n_{i+1/2}}{(\tilde{u}^n_{i+1/2})^2-\tilde{a}^2_{i+1/2}}\,(Z_{i+1}-Z_i) +$$

$$+\frac{\tilde{M}^n_{i+1/2}\ln(S_0)_{i+1/2}}{(\tilde{u}^n_{i+1/2})^2-\tilde{a}^2_{i+1/2}}\,(a^2_{i+1}-a^2_i)$$

and then, for instance, $W^*_{i+1/2}(0^-, W^n_i, W^n_{i+1}) = (Z_i, \Psi_i, M^{n,-}_{i+1/2}, D^n_{i+1/2})^t$. Adding the variables Z and Ψ in the system (22) produced upwinding terms:

$$g\,\tilde{M}^n_{i+1/2}\,(Z_{i+1}-Z_i) \quad \text{and} \quad \tilde{M}^n_{i+1/2}\ln(S_0)_{i+1/2}\,(a^2_{i+1}-a^2_i).$$

Considering the two last components of (23) we get our explicit first order scheme under the form:

$$\frac{U^{n+1}_i - U^n_i}{\Delta t} + \frac{F^{n,-}_{i+1/2} - F^{n,+}_{i-1/2}}{h_i} = H^n_i \quad 1 \le i \le N, \quad n \ge 0. \tag{25}$$

where

$$F^{n,\pm}_{i+1/2} = F(U^*_{i+1/2}(0^\pm, U^n_i, U^n_{i+1}))$$

with

$$U^*_{i+1/2}(0^\pm, U^n_i, U^n_{i+1}) = (M^{n,\pm}_{i+1/2}, D^n_{i+1/2})^t$$

and

$$H^n_i = -g\,K(A_i)\,\frac{D^n_i\,|D^n_i|}{M^n_i} = H(U^n_i).$$

Practically, with $\beta = 5.0\;10^{-10}\,m^2/N$ and in the undeformable case, the (CFL) condition gives $\Delta t \le 0.7\,10^{-3}\,\Delta x$. This severe restriction is a motivation for the construction of an implicit scheme.

3.2 First order implicit scheme

A fully implicit scheme based on the previous approach would write

$$\frac{U_i^{n+1} - U_i^n}{\Delta t} + \frac{F_{i+1/2}^{n+1,-} - F_{i-1/2}^{n+1,+}}{h_i} = H_i^{n+1} \tag{26}$$

with

$$F_{i+1/2}^{n+1,\pm} = F(U_{i+1/2}^*(0^\pm, U_i^{n+1}, U_{i+1}^{n+1})) \tag{27}$$

$$H_i^{n+1} = -g\, K(A_i)\, \frac{D_i^{n+1} \left| D_i^{n+1} \right|}{M_i^{n+1}} = H(U_i^{n+1}). \tag{28}$$

It would obviously be of high cost and not easily extended to second order. Another approach (see [11,9]) consists in linearizing F and the source term around their values at time t_n. Then we get, instead of (26)-(27)-(28)

$$\frac{U_i^{n+1} - U_i^n}{\Delta t} + \frac{\tilde{F}_{i+1/2}^{n+1,-} - \tilde{F}_{i-1/2}^{n+1,+}}{h_i} = \tilde{H}_i^{n+1} \tag{29}$$

with

$$\begin{aligned}
\tilde{F}_{i+1/2}^{n+1,\pm} &= F_{i+1/2}^{n,\pm} + JF\left(U_{i+1/2}^*(0^\pm, U_i^n, U_{i+1}^n)\right) \cdot \\
&\quad \cdot \left(U_{i+1/2}^*(0^\pm, U_i^{n+1}, U_{i+1}^{n+1}) - U_{i+1/2}^*(0^\pm, U_i^n, U_{i+1}^n)\right) \\
\tilde{H}_i^{n+1} &= H_i^n + JH(U_i^n) \cdot (U_i^{n+1} - U_i^n)
\end{aligned}$$

Thanks to the homogeneity property of the flux function F,

$$JF(U) \cdot U = F(U)$$

the numerical flux is given by:

$$\tilde{F}_{i+1/2}^{n+1} = JF(U_{i+1/2}^*(0^\pm, U_i^n, U_{i+1}^n)) \cdot (U_{i+1/2}^*(0^\pm, U_i^{n+1}, U_{i+1}^{n+1})) \tag{30}$$

At this stage (29) is a linear system of $2N$ equations and $2N + 4$ scalar unknowns because the upstream and downstream states U_0^{n+1} and U_{N+1}^{n+1} have to be determined. In the next subsection we specify our procedure to close this system.

Lastly, let us explain briefly how to deal with a deformable pipe. The cross area A_i^n being known at time t_n in mesh m_i, the source term

$$-\frac{1}{4}\frac{\partial_t A}{A}\,(\partial_x \delta_0)^2\; U$$

is discretized by

$$\frac{k_i^n (\partial_x \delta_0)_i^2}{4\, A_i^n \Delta t}\,(M_i^{n+1} - M_i^n) \begin{pmatrix} M_i^n \\ D_i^n \end{pmatrix}$$

according to the following time discrete version of the equation (14)

$$A_i^{n+1} = A_i^n + k_i^n\,(M_i^{n+1} - M_i^n) \tag{31}$$

where we set:

- $k_i^n = \dfrac{\delta_i^n}{e\,E\,\cos\phi(x_i)}\,(a_i^n)^2$,
- δ_i^n diameter asociated to A_i^n, and
- $a_i^n = \dfrac{c}{\sqrt{1 + \dfrac{\delta_i^n}{\beta\, e\, E\,\cos\phi(x_i)}}}$.

This leads to a minor modification of the system arising from (29).
Notice that it is convenient, in the source term $H(U_i^n)$, to replace $K(A_i)$ by $K(A_i^n)$ and in the matrix $\tilde{J}$ to replace $\tilde{a}_{i+1/2}^2$ by $(\tilde{a}^n)_{i+1/2}^2 = \dfrac{(a_i^n)^2 + (a_{i+1}^n)^2}{2}$.

The cross area A is then updated through (31). Notice that the computation of A allows us to get the pressure via $\rho = M/A$ and the discharge $Q = D/\rho$.

3.3 Boundary conditions

In order to achieve the description of the implicit scheme, we present now a way to take the boundary conditions into account. We recall that the upstream and downstream state vectors (corresponding to $x_{1/2}$ and $x_{N+1/2}$) at time t_n are respectively denoted $U_0^n = \begin{pmatrix} M_0^n \\ D_0^n \end{pmatrix}$ and $U_{N+1}^n = \begin{pmatrix} M_{N+1}^n \\ D_{N+1}^n \end{pmatrix}$. ¿From a mathematical point of view, we must give as many scalar boundary conditions as incoming characteristic curves, that is one at each end of the pipe. For example $M_0^n = M(0, t_n)$ and $D_{N+1}^n = D(L, t_n)$ are given quantities or, more generally, we impose some condition $f_u(M, D, t) = 0$ at the upstream end and $f_d(M, D, t) = 0$ at the downstream end.

Numerically, the computation of the boundary fluxes (via the resolution of the

Riemann problem (24)) requires complete state vectors that one can consider as "exterior" values on fictive meshes. U_0^n and U_{N+1}^n play this role and are supposed to be known at time t_n. Thus the problem is to determine or estimate the boundary states U_0^{n+1} and U_{N+1}^{n+1} in (29).

Using an explicit characteristic method (for instance) is not convenient because it is subject to a CFL type condition. The method described below is an adaptation to the implicit scheme of those studied by Dubois [7] and Kumbaro [14] (see also [8]). It allows to update the boundary states using known values at the same level time, so it is naturally implicit. Let us recall the original procedure in the case of the upstream state, for instance.

We start with given interior vector states U_i^{n+1} $(1 \leq i \leq N)$ and any given relationship

$$f_u(M_0^{n+1}, D_0^{n+1}, t_{n+1}) = 0.$$

We have to build a complete boundary state using these data at the same level time and not at the previous one as in the characteristic method. The vector states W_0^{n+1} and W_1^{n+1} are expressed in the basis of eigenvectors of the matrix $\tilde{J}$ in (24) where we assume that $Z_0 = Z_1$ and $\Psi_0 = \Psi_1$ (notice that these eigenvectors depend on the unknown U_0^{n+1}):

$$W_0^{n+1} = \alpha_0^{n+1}\tilde{r}_1 + \beta_0^{n+1}\tilde{r}_2 + \gamma_0^{n+1}\tilde{r}_3 + \delta_0^{n+1}\tilde{r}_4$$

$$\text{and} \quad W_1^{n+1} = \alpha_1^{n+1}\tilde{r}_1 + \beta_1^{n+1}\tilde{r}_2 + \gamma_1^{n+1}\tilde{r}_3 + \delta_1^{n+1}\tilde{r}_4.$$

The classical BC method consists of connecting U_0^{n+1} to U_1^{n+1} by an unique jump through the incoming characteristic $x = \tilde{\lambda}_4\, t$, thus setting

$$\alpha_0^{n+1} = \alpha_1^{n+1}, \quad \beta_0^{n+1} = \beta_1^{n+1} \text{ and } \gamma_0^{n+1} = \gamma_1^{n+1}$$

or equivalently $D_1^{n+1} - D_0^{n+1} = (\tilde{u}_{1/2}^{n+1} + \tilde{a}_{1/2})(M_1^{n+1} - M_0^{n+1})$. Then we get U_0^{n+1} as the solution of the nonlinear system:

$$\begin{cases} D_1^{n+1} - D_0^{n+1} = (\tilde{u}_{1/2}^{n+1} + \tilde{a}_{1/2})(M_1^{n+1} - M_0^{n+1}) \\ f_u(M_0^{n+1}, D_0^{n+1}, t_{n+1}) = 0. \end{cases} \tag{32}$$

Applying this method for nonlinear boundary conditions (BC in brief) at time t_{n+1} is not compatible with the framework of linearised implicit method as described above as above. We propose to apply it at time t_{n+1} after a first step which consists in completing (29) with four linear equations thanks to a modified procedure that we present further. Solving the resulting system supplies a first estimate of interior and unknown boundary states, then we make use of the standard BC method. Our adaptation to the implicit scheme consists of two steps.

First step : we apply the previous procedure using the eigenvectors of the matrix $\tilde{J}$ at time t_n instead of time t_{n+1}. From (32) we get the linear equation (with unknowns M_0^{n+1} and D_0^{n+1}):

$$D_1^{n+1} - D_0^{n+1} = (\tilde{u}_{1/2}^n + \tilde{a}_{1/2})(M_1^{n+1} - M_0^{n+1}) \tag{33}$$

and we use a linearized version $f_u^{lin}(M_0^{n+1}, D_0^{n+1}, t_{n+1}) = 0$ of the upstream boundary condition (around the vector state U_0^n). Similarly for the downstrean state we get

$$D_{N+1}^{n+1} - D_N^{n+1} = (\tilde{a}_{N+1/2} - \tilde{u}_{N+1/2}^n)\,(M_{N+1}^{n+1} - M_N^{n+1}) \tag{34}$$

and $f_d^{lin}(M_{N+1}^{n+1}, D_{N+1}^{n+1}, t_{n+1}) = 0$.

The linear system arising from (29) is now completely determined.
Second step : equipped with interior vector states issued from the first step, we apply the standard BC method (32) at time t_{n+1}.

Remark 1 Commonly used boundary conditions are for instance an upstream constant total head and the downstream flow $Q(t)$ (as in the presented numerical results). The total load in the pipe is defined by $H = z + \dfrac{u^2}{2g} + p$, where z is the altitude (m), u the flow speed (m/s), p the relative pressure (m) expressed in equivalent water height defined by $p = \dfrac{c^2\,(\rho - \rho_0)}{\rho_0\, g}$. We impose at the entrance of the pipe with altitude z_0 a constant load H_0. Thus we get $\left(\dfrac{D_0^{n+1}}{M_0^{n+1}}\right)^2 + \dfrac{2M_0^{n+1}}{\beta\rho_0^2 A_0} = 2g(H_0 - z_0) + \dfrac{2}{\beta\rho_0}$ as boundary datum in (32). The downstream boundary condition is $Q_{N+1}^{n+1} = Q(t_{n+1})$ which writes $\dfrac{D_{N+1}^{n+1}\, A_{N+1}^{n+1}}{M_{N+1}^{n+1}} = Q(t_{n+1})$ with $A_{N+1}^{n+1} = A_{N+1}^n + k_{N+1}^n\,(M_i^{n+1} - M_i^n)$ and a suitable definition of k_{N+1}^n. A similar technique as above is then applied.

3.4 Space second order implicit scheme

The main inconvenience with usual Roe-type schemes (as the Godunov one) as well as the implicit scheme is that this type of discretisation is very diffusive. One way to improve the scheme is to perform a second order space discretisation (which can be coupled with a second-order Runge-Kutta time discretisation). This type of improvement (for explicit schemes) seems to be practically a relaxation of the CFL condition more than a better space approximation.

We recall in the following section the principle of the MUSCL method for a second order explicit space discretisation and we propose a linearly implicit version of this commonly used method to improve spatial approximation.

3.4.1 MUSCL method

The MUSCL method (Monotonic Upstream Scheme for Conservation Laws), due to Van Leer ([15]), is based on a "reconstruction" step which consists in constructing a piecewise linear function from cell-averages. Then we can solve new local Riemann problems extrapolating the averaged states in each cell: this method, quite simple to implement, is a natural extension of the previous scheme.

The steps are as follows (with the same notations as in the explicit scheme):

(1) From given cell-averages $U_i^n, \quad 1 \leq i \leq N$ at time t_n, define slope vectors $\Sigma_i^n = \begin{pmatrix} \Sigma_{i,1}^n \\ \Sigma_{i,2}^n \end{pmatrix}$

(2) On each cell $]x_{i-1/2}, x_{i+1/2}[$ define a piecewise linear approximate solution

$$U^n(x) = U_i^n + (x - x_i)\Sigma_i^n$$

(3) Compute fluxes:

$$F_{i+1/2}^{n,\pm} = F(U_{i+1/2}^*(0^\pm, U_i^{n,+}, U_{i+1}^{n,-}))$$

where

$$\begin{cases} U_i^{n,+} = U_i^n + \dfrac{h_i}{2}\Sigma_i^n \\ U_{i+1}^{n,-} = U_{i+1}^n - \dfrac{h_{i+1}}{2}\Sigma_{i+1}^n \end{cases}$$

(4) Compute updated cell-averages U_i^{n+1} applying (25).

The first step (slopes reconstruction) is crucial. A natural way would consist in using the central difference $\dfrac{U_{i+1}^n - U_{i-1}^n}{x_{i+1} - x_{i-1}}$ which is a second order approximation of $U'(x_i)$. In order to satisfy some monotonicity and TVD properties, we apply a limitation procedure, for instance the following classical one (see [12] for instance). For $k = 1, 2$ we set

$$\Sigma_{i,k}^n = minmod\left(\frac{U_{i+1,k}^n - U_{i,k}^n}{x_{i+1} - x_i}, \frac{U_{i,k}^n - U_{i-1,k}^n}{x_i - x_{i-1}}\right) \tag{35}$$

where the *minmod* function is defined over $\mathbb{R}^2$ by

$$minmod(a, b) = \begin{cases} \min(|a|, |b|)\, sgn(a) & \text{if } sgn(a) = sgn(b), \\ 0 & \text{else.} \end{cases}$$

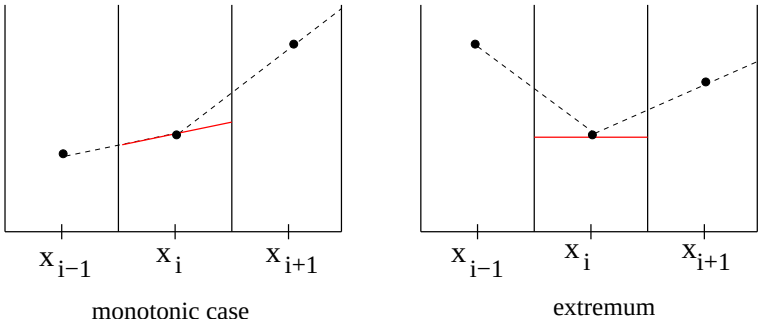

Fig. 3. *slopes reconstruction.*

3.4.2 An adaptation to the implicit scheme

A direct application of this method to the previous first order scheme would introduce non linearities due to slopes computations. Instead we propose the following procedure in three steps:

First step :

¿From the averaged states $U_i^n, \quad i = 1, ..., N$, at time t_n, we define the slope vectors Σ_i^n following (35). Then we compute at each interface $x_{i+1/2}$ the corresponding states $U_i^{n,+}$, $U_{i+1}^{n,-}$ and finally $U^*_{i+1/2}(0^{\pm}, U_i^{n,+}, U_{i+1}^{n,-})$.

Second step :

A first estimate $\tilde{U}_i^{n+1}$ of U_i^{n+1} is computed applying the first order scheme (29) together with the treatment of the boundary conditions as in section 3.3. We deduce a first estimate $\tilde{\Sigma}_i^{n+1}$ of the slopes Σ_i^{n+1}.

Third step :

The second order fully implicit scheme, would write under the form (26) with

$$\begin{aligned} F_{i+1/2}^{n+1,\pm} &= F(U^*_{i+1/2}(0^{\pm}, U_i^{n+1,+}, U_{i+1}^{n+1,-})) \\ H_i^{n+1} &= H(U_i^{n+1}) \ . \end{aligned}$$

The linear implicit second order scheme is obtained by linearizing $F_{i+1/2}^{n+1,\pm}$ around $U_i^{n,+}$ and $U_{i+1}^{n,-}$, by using in (24) a matrix $\tilde{J}$ associated to states $(U_i^{n,+}, U_{i+1}^{n,-})$ at time t_n instead of $(U_i^{n+1,+}, U_{i+1}^{n+1,-})$ and finally by using the estimated slope $\tilde{\Sigma}_i^{n+1}$ to compute $U_i^{n+1,+}$ and $U_{i+1}^{n+1,-}$. It leads to a scheme under the form:

$$\frac{U_i^{n+1} - U_i^n}{\Delta t} + \frac{\tilde{F}_{i+1/2}^{n+1,-} - \tilde{F}_{i-1/2}^{n+1,+}}{h_i} = \tilde{H}_i^{n+1} \tag{36}$$

with

$$\begin{aligned}
\tilde{F}_{i+1/2}^{n+1,\pm} &= JF(U_{i+1/2}^*(0^\pm, U_i^{n,+}, U_{i+1}^{n,-})) \cdot (U_{i+1/2}^*(0^\pm, U_i^{n+1,+}, U_{i+1}^{n+1,-})) \\
\tilde{H}_i^{n+1} &= H_i^n + JH(U_i^n) \cdot (U_i^{n+1} - U_i^n)
\end{aligned}$$

where

$$\begin{cases}
U_i^{n+1,+} = U_i^{n+1} + \dfrac{h_i}{2}\, \tilde{\Sigma}_i^{n+1} \\[2ex]
U_{i+1}^{n+1,-} = U_{i+1}^{n+1} - \dfrac{h_{i+1}}{2}\, \tilde{\Sigma}_{i+1}^{n+1}
\end{cases}$$

Finally the updated states U_i^{n+1} are solutions of the linear system arising from (36) combined with the equations (33)-(34) where M_1^{n+1}, D_1^{n+1}, M_N^{n+1} and D_N^{n+1} are respectively replaced with $M_1^{n+1,-}$, $D_1^{n+1,-}$, $M_N^{n+1,+}$ and $D_N^{n+1,+}$. The treatment of the boundary conditions is performed using (32) modified in a similar way. Finally, in the case of a deformable pipe, the procedure is the same as in the first order implicit scheme.

4 Numerical validation in the case of a constant radius circular pipe

We present now numerical results of a water hammer test. The pipe of circular cross-section of 2 m^2 and thickness 20 cm is 2000 m long. The altitude of the upstream end of the pipe is 250 m and the angle is 5°. The Young modulus is $23\,10^9$ Pa since the pipe is supposed to be built in concrete. The total upstream head is 300 m. The initial downstream discharge is 10 m^3/s and we cut the flow in 5 seconds. The number of mesh points is either 1000 or 150 depending on the tests and is presented for each of them. Let us define the piezometric line by:

$$piezo = z + \delta + p \;\text{ with } p = \frac{c^2\,(\rho - \rho_0)}{\rho_0\, g}\,.$$

4.1 Comparison with the solution of Allievi equations

To ensure that the model that we propose describes precisely flows in closed pipe-lines, we present a validation of it by comparing numerical results of the proposed model with the ones obtained by solving Allievi equations by the method of characteristics with the so-called `belier` code used by the Center in Hydraulics Engineering of Electricité De France (EDF) [21]. Our code is written in Fortran 77.

A first simulation of the water hammer test was done for a CFL coefficient equal to 1 (i.e. $CFL = 1$) and a spatial discretisation of 1000 mesh points (the mesh size is equal to 2 m). In the figure 4, we present a comparison between the results obtained by our first order scheme and the ones obtained by the "belier" code at the middle of the pipe: the behavior of the piezometric line and the discharge at the middle of the pipe. One can observe that the results for the proposed model are in very good agreement with the solution of Allievi equations. A little smoothing effect and absorption may be probably due to the first order discretisation type. It is the reason why we perform the same test, in the same condition ($CFL = 1$ and 1000 mesh points) with the second order scheme. The figure 5 shows that this smoothing effect is much less important with this second order scheme. It is the reason why in the following numerical results, we consider the second order scheme with a CFL condition equal to 1 as the reference solution.

4.2 Influence of the CFL coefficient

The purpose of our scheme is to perform a solution with a not accurate spatial detail but with very low computational costs. As argued before, we choose to perform a linear implicit spatial discretisation (first order and second order) to get rid of the CFL condition imposed for the stability of explicit discretisation of hyperbolic systems of partial differential equations. Since the proposed space discretisation is only linear implicit (to keep a low CPU time), we can expect a deterioration of the results for $CFL > 1$. Therefore, we performed the same test as above for different CFL coefficients and 1000 mesh points. We present in the figure 6, the same quantities (piezometric line and discharge) at the middle of the pipe for the second order space discretisation scheme. One can observe that even for $CFL = 10$, the results are good from the point of view of the maximum pressure calculation and that the second order implicit discretisation is very stable in regard of the time discretisation. The very good behavior of this scheme from the point of view of the time discretisation is a very good argument for using it, even though we must solve at each time-step a linear system (which contains only 6 diagonals). Moreover, we wanted

to study the behavior of the scheme from the point of view of the spatial discretisation. Thus we perform the same test for different CFL coefficients and for only 150 mesh points (the mesh size is then 13,33 m). Before doing this test, we suspected a bad behavior for a coarse space mesh and great CFL coefficients since the scale of the physical effects of a water hammer is very small against this space mesh size and this time-step. Figure 7 shows the behavior of the second order scheme for a coarse grid discretisation and for different CFL numbers. A great smoothing effect is present but it seems that the highest pressure value is well computed.

Nevertheless, the hydraulics engineers are interested in the value of the highest pressure in the pipe to make a good evaluation of the size and the strength of the pipe. Therefore we present in table 1 the highest piezometric line computed in the pipe and the relative error with the highest piezometric line computed by the code `belier` for the preceding water hammer test, $P_{max} = 688.442$. The relative error is very small and therefore even for a coarse mesh and a great CFL coefficient, the highest piezometric level is "well" computed in a very small CPU time.

CFL	1	2	5	10
$N_x = 1000$	688 **0.04%**	685 **0.4%**	680 **1.2%**	673 **2.2%**
$N_x = 150$	677 **1.7%**	669 **2.8%**	655 **4.9%**	638 **7.3%**

Table 1
Highest piezometric level and relative error (in bold).

4.3 Case of contracting or expanding sections

In order to illustrate the effect of the variations of the sections and the important contribution of the term of geometry (terms $a^2 \dfrac{M}{A} \partial_x S_0$ and $M \partial_x a^2$ in equation (13)), we consider the case of an immediate flow shut-down in a frictionless cone-shaped pipe. We thus computed the waterhammer pressure rise at the middle of the pipe ΔH and relate it to the pressure rises calculated for an equivalent pipe segment ΔH_{eq} as presented in [1,19].

Let us hereby recall how do we transform a real pipe with expanding or contracting sections to an equivalent pipe of constant dimension. The similarity conditions should be preserved in order to transform a pipe with expanding or contracting sections to an equivalent uniform pipe segment. These conditions imply that the following properties should not change in the equivalent pipe segment, compared to the real pipe of the same length L :

(1) inertia forces due to the same way of flow shutdown,
(2) pressure wave propagation time.

Condition (1) leads to the following formula for the equivalent cross-sectional area S_{eq} of the pipe segment :

$$S_{eq} = \frac{L}{\int_0^L \frac{dx}{S(x)}}$$

The equivalent pressure wave speed a_{eq} can be found from the condition (2):

$$a_{eq} = \frac{L}{\int_0^L \frac{dx}{a(x)}}$$

We thus perform tests of flows shut-down at downstream end of a cone-shaped pipe of lenght $L = 1000$ m, the upstream diameter D_1 being always equal to 1 m whereas the downstream diameter D_2 varies. We use 100 mesh points and the CFL number is chosen equal to 0.8. Before the shut-down, the downstream discharge is $1m^3/s$. Figure 8 shows the ratio $\Delta H/\Delta H_{eq}$ versus the ratio D_1/D_2. The model and the proposed finite volume discretisation shows a very good agreement with the equivalent pipe theory.

4.4 Effect of the pipe deformation

To see the effect of the deformation of the pipe on the values of the piezometric line and the discharge, we perform the same water hammer test where we take into account the deformation of the pipe. Let us recall that from equation (12) the speed of the sound is in this case non constant and depends on the Young's modulus, the thickness of the wall and the diameter of the pipe. We present in the figure 9 the piezometric line, the discharge and the diameter of the pipe at the middle of the pipe computed by the second order scheme with $CFL = 1$ and 1000 mesh points.

One can remark that in the deformable case, the pressure is less high since the pipe absorbs a great part of the stress and the frequency of the smaller

(since the speed of the sound is smaller in the deformable case). These results must be viewed as an illustration of our model.

Acknowledgments. The authors thank EDF-CIH (France) for helpfull discussions and supplying us the numerical results of the `belier` code. They also thank the referees for their appropriate advises in the presentation of this article.

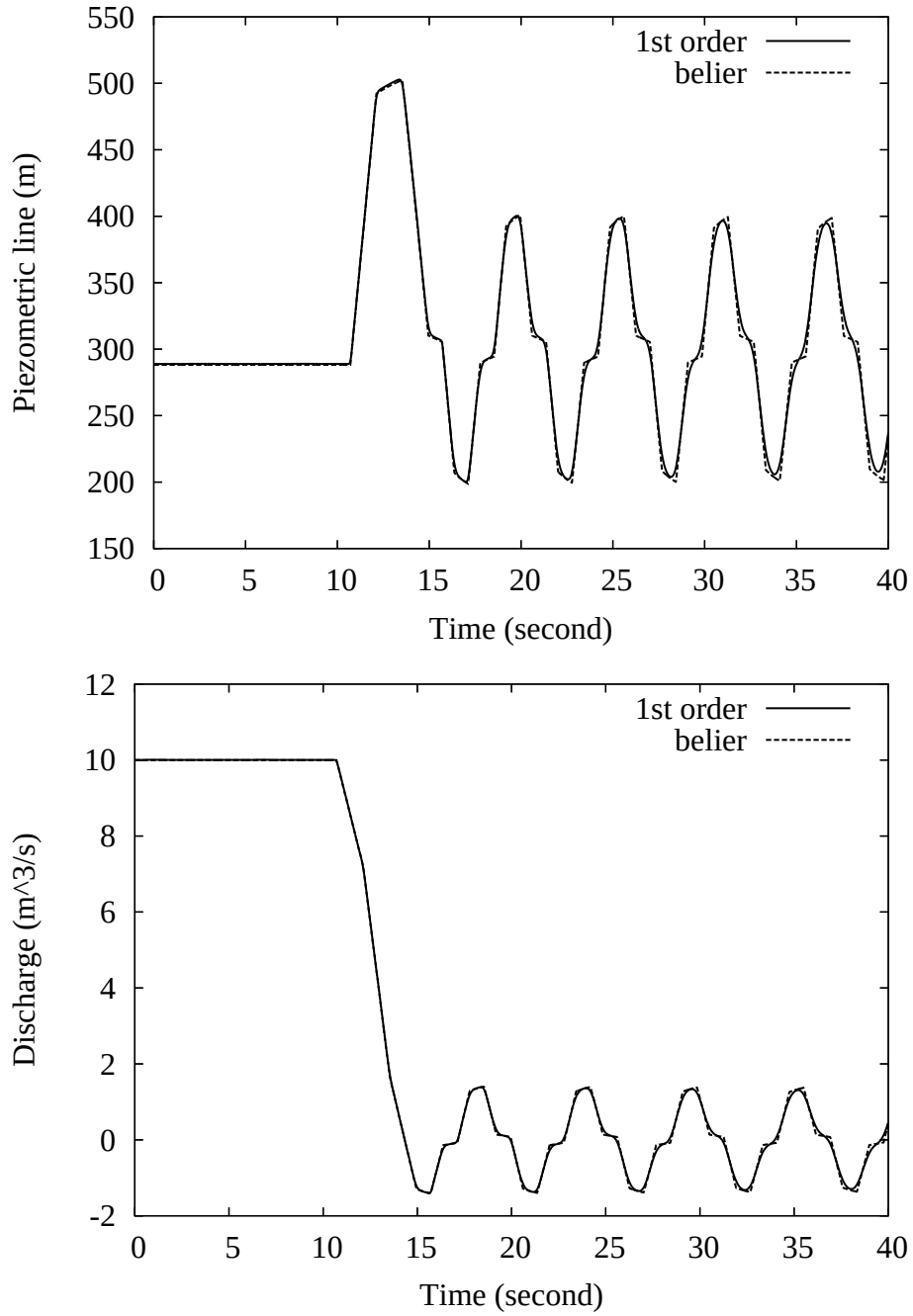

Fig. 4. Validation of the model: 1st order scheme
Piezometric line (top) and discharge (bottom) at the middle of the pipe

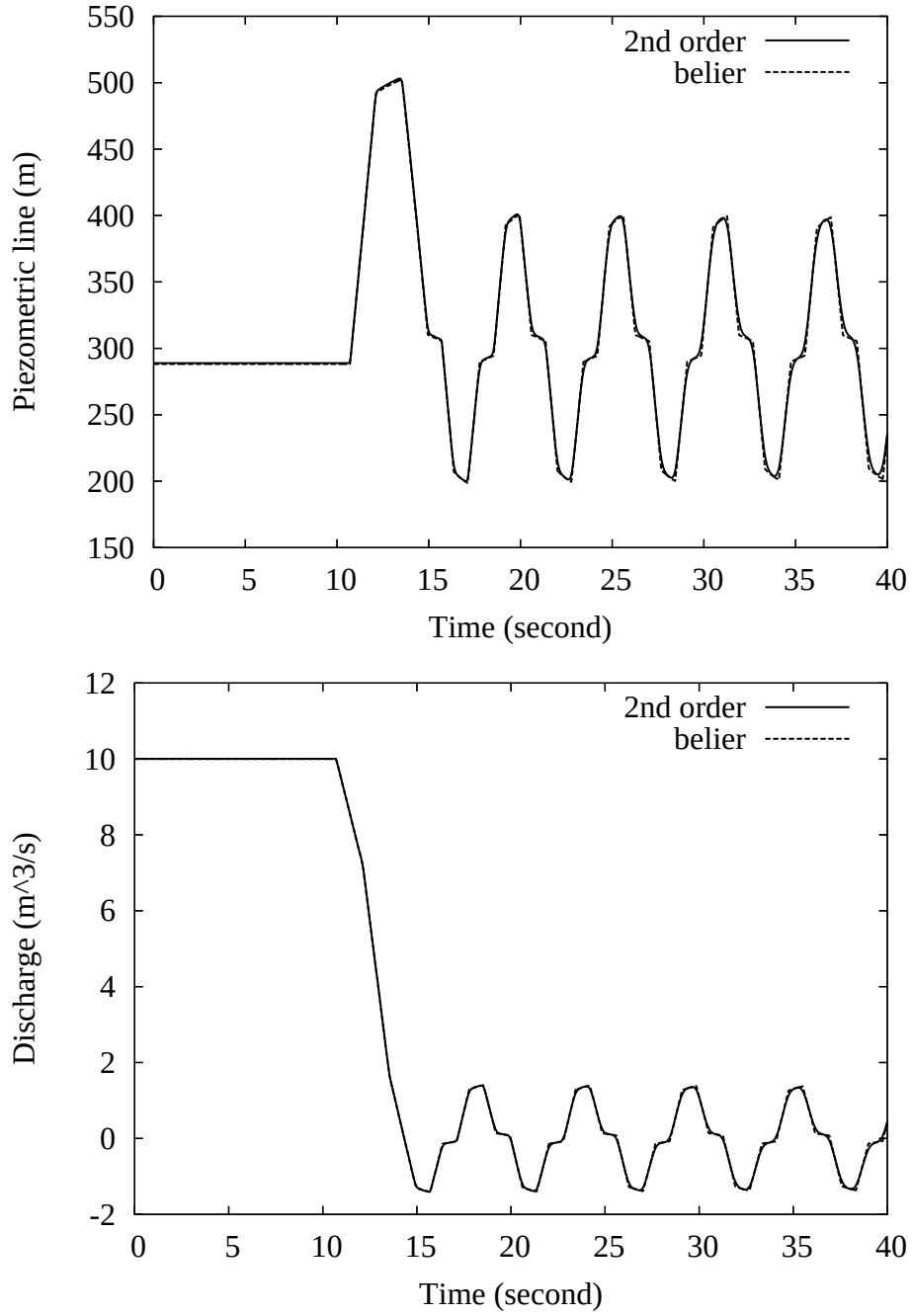

Fig. 5. Validation of the model: 2nd order scheme
Piezometric line (top) and discharge (bottom) at the middle of the pipe

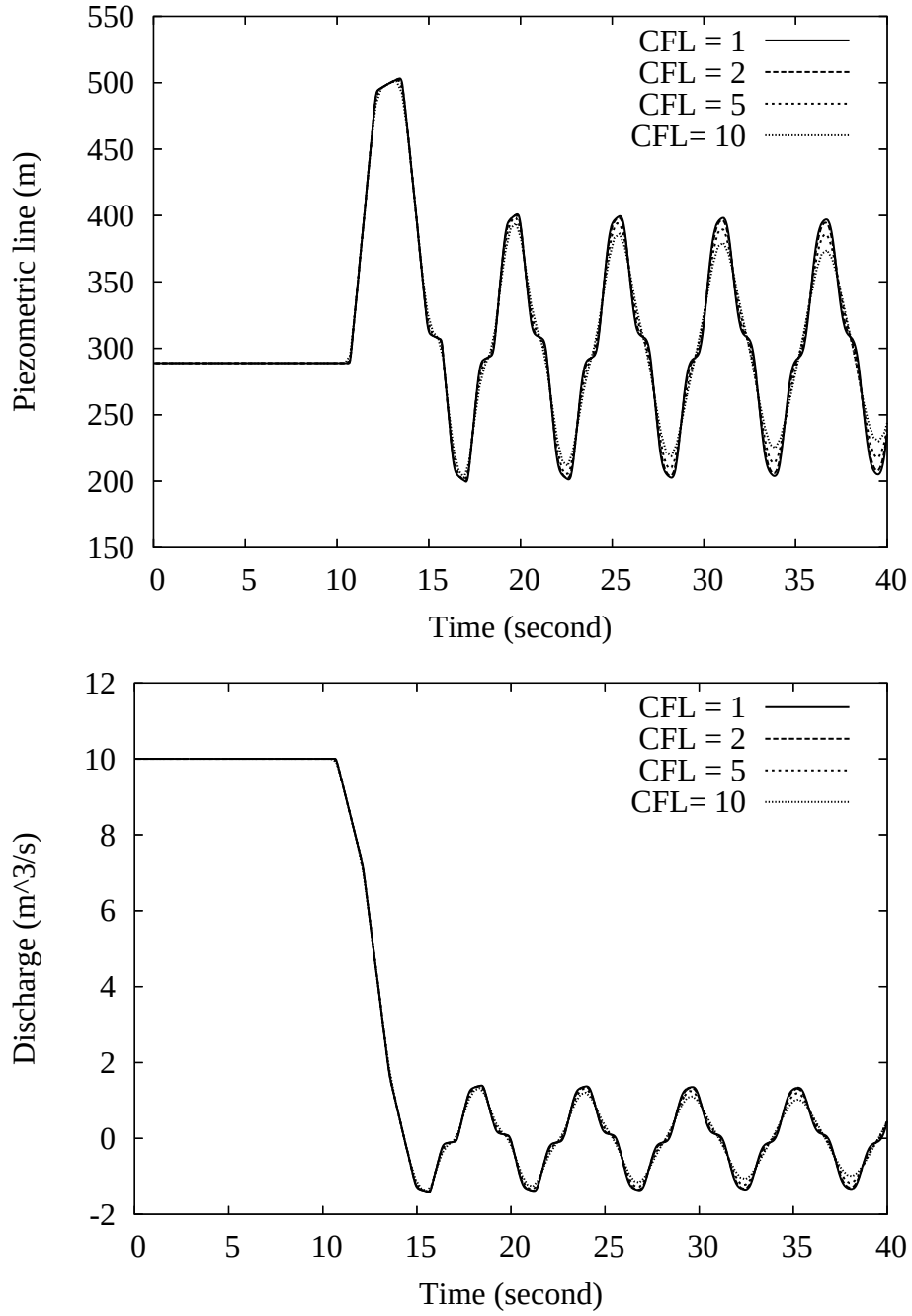

Fig. 6. Numerical behavior for a fine space mesh and different CFL numbers Piezometric line (top) and discharge (bottom) at the middle of the pipe

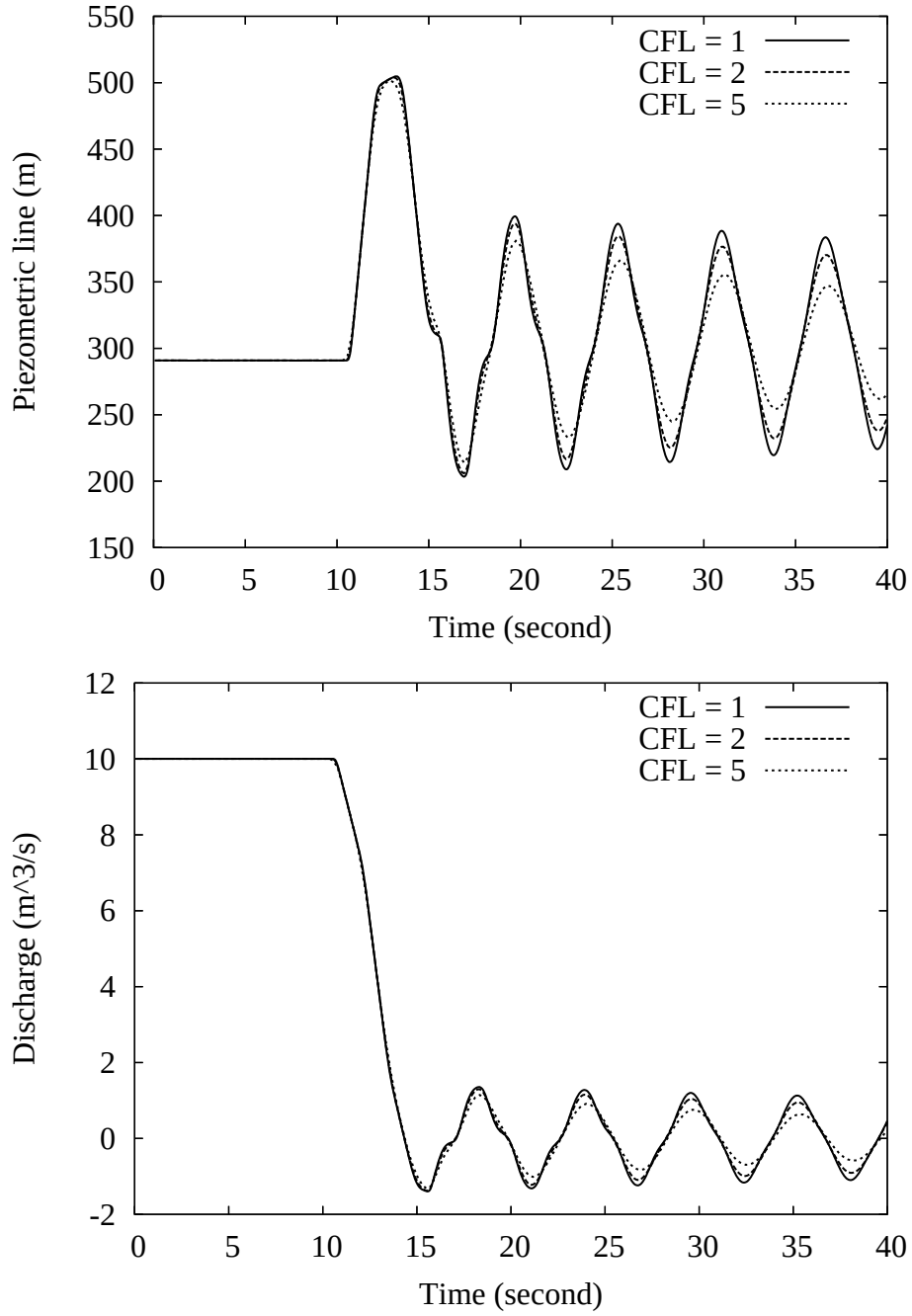

Fig. 7. Numerical behavior for a coarse space mesh and different CFL numbers
Piezometric line (top) and discharge (bottom) at the middle of the pipe

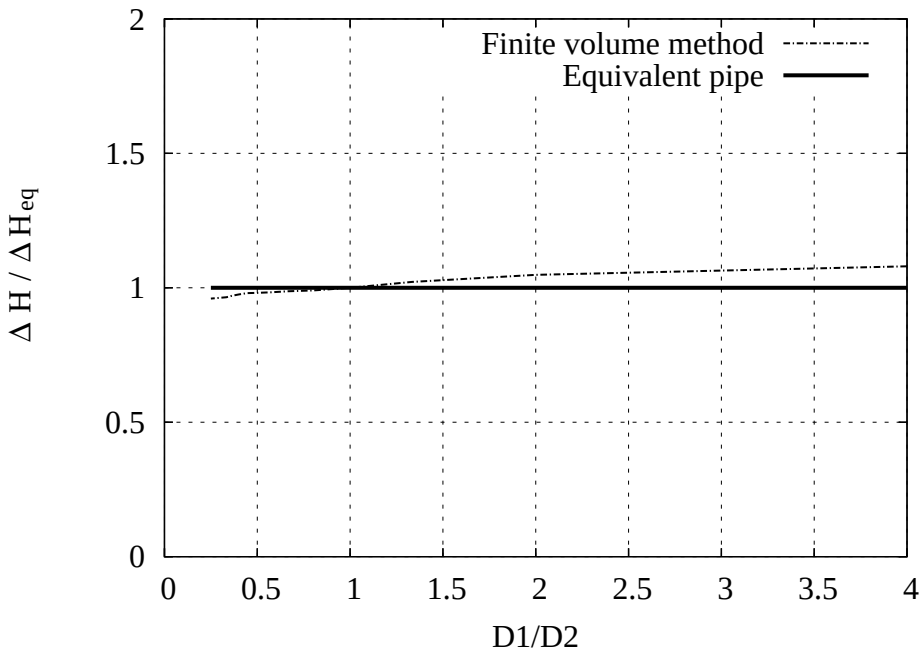

Fig. 8. Comparison in the prediction of pressure rises in cone-shaped pipes between the present method and the equivalent pipe method

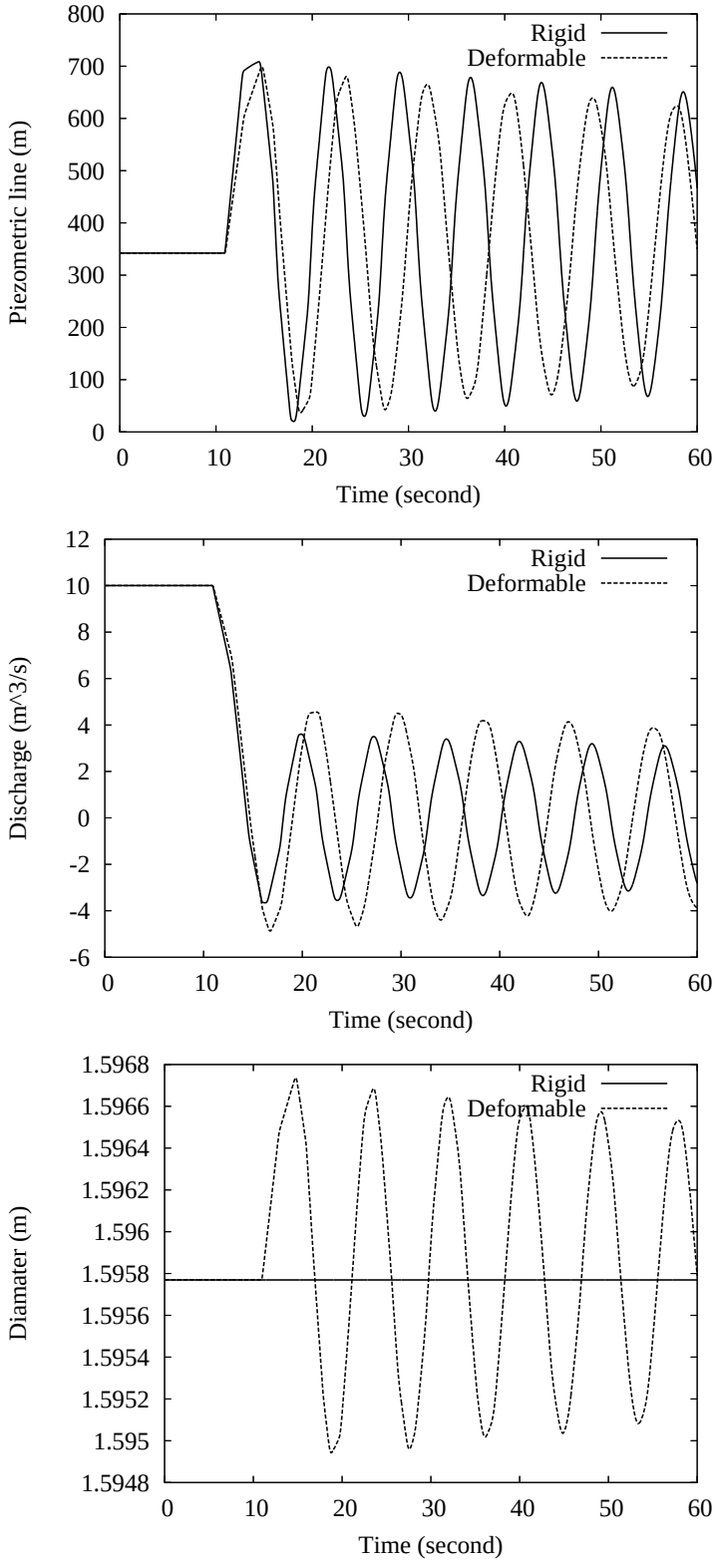

Fig. 9. Influence of the pipe deformation
Piezometric line (top), discharge (middle) and diameter (bottom) at the middle of the pipe

A Nomenclature

c	=	pressure wave speed in a rigid pipe	a	=	pressure wave speed
β	=	inverse of the bulk modulus elasticity	g	=	gravitational acceleration
P_a	=	athmospheric pressure	P	=	pressure of liquid
ρ_0	=	liquid mass density at pressure P_a	ρ	=	mass density at press. P
Ω	=	cross section, with boundary $\partial\Omega$	A	=	pipe cross-sectional area
ω	=	center of Ω	$\vec{m}$	=	$\overrightarrow{\omega m}$, where $m \in \partial\Omega$
x	=	longitudinal coordinate	t	=	time
S	=	function of x and P s.t. $A = S(x, P)$	u	=	x-liquid mean velocity
$\vec{U}$	=	velocity	$\vec{V}$	=	velocity in the Ω-plane
p	=	elev. of hydr. grade line $(= \frac{P}{\rho_0 g})$	Q	=	discharge $(= A\,u)$
L	=	pipe length	z	=	elevation of pipe bottom
E	=	pipe wall modulus of elasticity	e	=	pipe wall thickness
$\vec{N}$	=	outward unit normal vector	δ	=	pipe inner diameter
ϕ	=	angle between $\vec{n}$ and $\vec{N}$	P_m	=	pipe inner perimeter
R_h	=	hydraulic radius $(= \frac{A}{P_m})$	S_f	=	friction
K_s	=	Strickler coefficient	θ	=	slope of pipe axis
$\vec{n}$	=	outward unit normal vector in the Ω-plane			

References

[1] A. Adamkowski. Analysis of transient flow in pipes with expanding or contracting sections. *ASME J. of Fluid Engineering*, 125:716–722, 2003.

[2] C. Bourdarias and S. Gerbi. A finite volume scheme for a model coupling free surface and pressurised flows in pipes. *to appear in J. Comp. Appl. Math.*

[3] C. Bourdarias and S. Gerbi. An implicit finite volumes scheme for unsteady flows in deformable pipe-lines. In R. Herbin and D. Kröner, editors, *Finite Volumes for Complex Applications III: Problems and Perspectives*, pages 463–470. HERMES Science Publications, 2002.

[4] C. Bourdarias and S. Gerbi. Etude et mise en oeuvre d'un schéma de type Roe implicite pour les écoulements mixtes à surface libre et en charge. Research report, EDF-CIH and Université de Savoie, 2003.

[5] H. Capart, X. Sillen, and Y. Zech. Numerical and experimental water transients in sewer pipes. *Journal of hydraulic research*, pages 659–672, 1997.

[6] J.A. Cunge and M. Wegner. Intégration numérique des équations d'écoulement de Barré de Saint Venant par un schéma implicite de différences finies. *La Houille Blanche*, pages 33–39, 1964.

[7] F. Dubois. An introduction to finite volumes. In O. Pironneau and V. Shaidurov, editors, *Computational Methods and Algorithms (Related chapters)*, volume 2.6 of *Encyclopedia of Mathematical Sciences*. Encyclopedia of Life Support Systems, 2001.

[8] R. Eymard, T. Gallouet, and R. Herbin. The finite volume method. In P. Ciarlet and J.L. Lions, editors, *Handbook of numerical analysis*, pages 713–1020. North Holland, 2000. This paper appeared as a technical report four years ago.

[9] T. Gallouet. Rough schemes for complex hyperbolic systems. In F. Benkhaldoun R. Vilsmeier and D. Hanel, editors, *Finite Volumes for Complex Applications II: Problems and Perspectives*. HERMES Science Publications, 1996.

[10] T. Gallouet, J. M. Hérard, and N. Seguin. Some approximate Godunov schemes to compute shallow-water equations with topography. *Comput. Fluids*, 32:479–513, 2003.

[11] T. Gallouet and J.M. Masella. Un schéma de Godunov approché. (A rough Godunov scheme). *C. R. Acad. Sci., Ser. I*, 323(1):77–84, 1996.

[12] E. Godlewski and P.A. Raviart. *Hyperbolics systems of conservation laws*, volume 3/4 of *Mathématiques & Applications*. Ellipses, Paris, 1991.

[13] J.M. Greenberg and A.Y. LeRoux. A well balanced scheme for the numerical processing of source terms in hyperbolic equation. *SIAM J. Numer. Anal.*, pages 1–16, 1996.

[14] A. Kumbaro. *Modélisation, analyse mathématique et numérique des modèles bi-fluides d'écoulements diphasiques.* PhD thesis, Université Paris XI, 1993.

[15] B. Van Leer. Towards the ultimate conservative difference scheme. v: Upstream-centered finite difference schemes for ideal compressible flow. *J. of Comp. Ph*, 32:101–136, 1979.

[16] P.L. Roe. Some contributions to the modelling of discontinuous flow. In B. E. Engquist, S. Osher, and R. C. J. Somerville, editors, *Large-scale computations in fluid mechanics. Part 2. Proceedings of the fifteenth AMS-SIAM summer seminar on applied mathematics held at Scripps Institution of Oceanography, La Jolla, Calif., June 27–July 8, 1983*, volume 22 of *Lectures in Applied Mathematics*, pages 163–193. American Mathematical Society, 1985.

[17] A. Y. Le Roux and M. N. Le Roux. Convergence d'un schéma à profils stationnaires pour les équations quasi linéaires du premier ordre avec termes sources. *C. R. Acad. Sci.*, Sér. I, Math. 333(7):703–706, 2001.

[18] C.S.S. Song, J.A. Cardle, and K.S. Leung. Transient mixed-flow models for storm sewers. *Journal of Hydraulic Engineering, ASCE*, pages 1487–1503, 1983.

[19] V.L. Streeter, E.B. Wylie, and K.W. Bedford. *Fluid Mechanics.* McGraw-Hill, 1998.

[20] D.C. Wiggert and M.J. Sundquist. Fixed-grid characteristics for pipeline transients. *Journal of the Hydraulics division*, 103(12):1403–1416, 1977.

[21] V. Winckler. Logiciel BELIER4.0. Notes de principes. Technical report, EDF-CIH, Le Bourget du Lac, France, 1993.